Selective growth of Co nanoislands on an oxygen-patterned Ru(0001) surface

H. F. Ding,[1,*] A. K. Schmid,[2] D. J. Keavney,[3] Dongqi Li,[1] R. Cheng,[1] J. E. Pearson,[1] F. Y. Fradin,[1] and S. D. Bader[1]
[1]*Materials Science Division and Center for Nanoscale Materials, Argonne National Laboratory, 9700 South Cass Avenue, Argonne, Illinois 60439*
[2]*Materials Sciences Division, Lawrence Berkeley National Laboratory, 1 Cyclotron Road, Berkeley, California 94720*
[3]*Advanced Photon Source, Argonne National Laboratory, 9700 South Cass Avenue, Argonne, Illinois 60439*
(Received 22 February 2005; published 6 July 2005)

We present a combined low energy electron microscopy and photoemission electron microscopy study of Co nanoislands grown on pure and partially oxidized Ru(0001) surfaces at 650–850 K. When Co is deposited on pure Ru(0001) at the temperature above ≈700 K, it first forms a wetting monolayer and then Co nanoislands abruptly nucleate. Partial oxidization of the clean Ru(0001) surface gives rise to large rhombus-shaped Ru–O patches (of 10 μm scale). On this surface at ≈730 K the Co islands form with different density in the Ru and Ru–O regions, and at ≈800 K the Co islands only grow in the pure Ru regions. We attribute this selectivity to differences in the temperature dependence of the sticking coefficients for Co on the pure Ru and Ru–O regions.

DOI: 10.1103/PhysRevB.72.035413 PACS number(s): 81.16.Dn, 61.46.+w, 68.37.Yz, 68.37.Nq

I. INTRODUCTION

Lateral nanostructures are of interest to explore low-dimensional physics and create new functional materials. Fabrication of lateral nanostructures by self-assembly is appealing because it is potentially adaptable to industrial processing.[1] Self-assembly has been realized as quantum dots with high uniformity and relatively ordered dot arrays in many semiconductor systems.[2] In metallic systems, self-assembly has been observed as nanowires via step decoration[3–7] or dots with thickness of one or a few monolayers (ML).[8–13] Recently, we reported the self-assembly of several nanometer thick Co dots/antidots.[14] In this paper, we address the formation mechanism of such self-assembly by means of low energy electron microscopy (LEEM) and photoemission electron microscopy (PEEM). A sharp nucleation process of the islands is revealed during the growth. We also compare the formation of Co nanodots grown on pure Ru(0001) and partially oxidized Ru(0001). The oxidation of Ru has been discussed extensively in terms of catalytical properties and the rich phases that may coexist, including physisorption and chemisorption of oxygen, surface oxide, buried oxides, and subsurface oxygen.[15–20] In this paper, we discuss a partially oxidized Ru(0001) surface formed at high temperature and high vacuum with residual oxygen to form a 10-μm-scale rhombus pattern. At ≈730 K, Co islands of different density form in the Ru and Ru–O areas. At ≈800 K, Co islands only appear outside of the Ru–O patterned areas. The formation mechanism is discussed in terms of the sticking coefficients and atomic mobilities.

II. EXPERIMENT

Our experiments were performed in an ultrahigh vacuum system (UHV) with a base pressure of 5×10^{-11} mbar. Single crystalline Ru(0001) substrates were cleaned by cycles of flash heating to ≈1300 K in an atmosphere of high purity oxygen at 1×10^{-7} mbar. Auger electron spectroscopy was used to ensure that sample surfaces were free of carbon contamination. After cleaning, the substrates were flash heated again under UHV. When the final flash temperature is above ≈1600 K, the residual oxygen is completely removed. In the temperature range of ≈1300–1500 K, residual oxygen partially oxidizes the Ru(0001) surface. During Co depositions, the substrate temperature was stabilized at various values in the range of ≈650–850 K. Electron beam evaporation of high-purity Co was used with a growth rate of typically 0.1–0.2 ML/min, while the background pressure remained $<2\times10^{-10}$ mbar. During deposition the growth of Co nanoislands was simultaneously monitored by LEEM, using an image acquisition rate of typically 1 frame/s.

In LEEM, a beam of low-energy electrons is backscattered at the sample surface and is collected to form images on a phosphor screen. Many surface properties, including morphology and chemical composition, give rise to the contrast in these images.[21] In the present study we monitor growth morphology and dimensions of the Co islands, for this we use mainly step-edge contrast and the reflectivity differences between pure Ru and Ru covered with Co layers of various thicknesses. Step-contrast arises because electrons backscattered from neighboring terraces interfere with each other at the step edges. Depending on the electron beam energy and the height of steps, this interference is often not perfectly constructive, in that case the images of steps appear as lines that are darker than the surrounding flat terraces. This type of step contrast is discussed in detail in the literature.[22] In addition, by virtue of its origin in electron diffraction phenomena, the energy dependent electron reflectivity of surfaces depends on which atomic species are present, crystalline structure, and overlayer thickness. We found that for our purpose it was convenient to use an electron beam energy of 5.3 eV. In that case the reflectivity of pure Ru is high, the reflectivity of Ru covered with a single monolayer of Co is visibly lower, and thicker films of Co produce even darker contrast.

In addition, PEEM is used to obtain chemically resolved images.[23,24] In PEEM, a soft x-ray beam is incident on the sample at 25° above the film plane, and the photoemitted electrons are imaged, providing a spatial map of the photo-

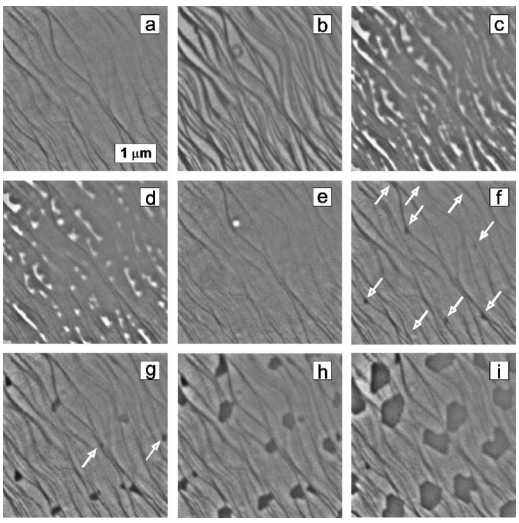

FIG. 1. Series of LEEM images during the initial Co growth on clean Ru(0001) at 850 K: (a) substrate; (b) 0.35 ML; (c) 0.8 ML; (d) 0.9 ML; (e) 0.98 ML; (f) 1.08 ML; (g) 1.16 ML; (h) 2 ML; and (i) 6 ML; The arrows indicate the nucleation position of Co islands. All images have 3.9 μm field of view.

electron yield. Chemical contrast is obtained by exciting at the Co $2p-3d$ resonance (778.1 eV) and subtracting a below-resonance background image. Magnetic images are derived using the x-ray magnetic circular dichroism effect from the difference of two on-resonance images taken with left- and right-circularly polarized x rays. The magnetic contrast in PEEM depends on the magnetization projection along the x-ray beam direction. With 25° angle of incidence, the images are sensitive to both in-plane and perpendicular magnetization but with the reduced sensitivity in the perpendicular direction. The PEEM measurement is performed at room temperature.

III. RESULTS AND DISCUSSION

We find that Co deposition at a substrate temperature below 700 K results in the growth of continuous films up to 3 or 4 ML. Above ≈700 K, Co first forms a 1-ML-thick wetting layer; islanding then starts with continued deposition. The lateral sizes of the Co islands are usually in the range of 20–800 nm, depending on Co dose and substrate temperature. Figure 1 presents an example of the initial growth obtained at ≈850 K. The substrate image, Fig. 1(a), shows many dim streaks on the gray background, which are step edges of the substrate. Many of the step edges have single atomic height, and locally they often bunch together and their combined contrast becomes stronger. Our detailed inspection reveals that ≈72 steps are resolved in the image, this implies that the average width of atomically flat terraces in this region of the surface is on the order of ≈70 nm. Figure 1(b) shows a sample with 0.35±0.02 ML Co [with the growth rate we use, ≈60 images are taken during the 1-ML-equivalent (MLE) deposition]. The step edge streaks widen, indicating that one-monolayer-thick ribbons of Co are growing outward from the substrate step edges. As the

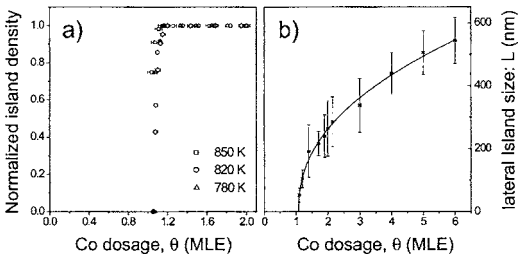

FIG. 2. (a) Co dosage dependence of the normalized Co island density at the indicated growth temperatures, (b) Co dosage dependence of the Co lateral size at 850 K. The symbols are experimental data, and the solid line is a fit.

growth continues, wave-like undulations develop in the edges of the advancing Co monolayer [see Figs. 1(c) and 1(d)]. The Co growth continues in this mode until a perfect, single-monolayer-thick Co film is complete. This is seen in the image with 0.98 ML Co, Fig. 1(e), which appears almost identical with the substrate image [Fig.1(a)] except for one white dot on the upper-left (the dot is likely a small island-shaped terrace of the original Ru surface). This indicates that the first ML wets the substrate, which is consistent with the fact that the surface energy of Co(0001) (2.7 J cm^{-2}) is lower than that of Ru(0001) (3.4 J cm^{-2}).[25] The relative values of surface energies, and possibly the contribution of strain energy due to the large lattice mismatch of 7.3% between Co and Ru, prevents layer-by-layer growth in this system and leads to the growth of 3D islands with further deposition (Stranski–Krastanov growth mode). Figures 1(f) and 1(g) present the nucleation process of the Co islands, as marked with arrows. Typically, the islands nucleate near step bunches. The location of the islands is possibly related to the presence of local defects or strain distribution after the flashing. The nucleation occurs within a very narrow thickness range. Below 1.08±0.02 ML, no islands are found within our resolution limits. Above 1.16±0.02 ML, no new islands nucleate but instead existing ones expand [see Figs. 1(h) and 1(i)].

To quantify the sharp nucleation process, we plotted the normalized dot density as a function of dosage for different substrate temperatures in Fig. 2(a). From the plot, we can see that, in the temperature range 780–850 K, island nucleation occurs from 1.05 to 1.18 ML. With further increased dosage, island nucleation is arrested, and instead the islands expand. Figure 2(b) shows the average lateral island dimension L as a function of Co dosage θ. The solid line shows the best-fit to the measured size during the growth using the expression: $L=L_0(\theta-\theta_c)^P$, where $L_0=271\pm6$ nm, $\theta_c=1.07\pm0.02$ MLE, and $P=0.44\pm0.02$. Under ideal condition, we might expect to find a value of $P=0.5$ in the case of 2D growth or $P=0.33$ in the case of 3D growth. The fitted value does not match either of these ideal values. The reason is that the growth that we observe is slightly different from the simple cases. By comparing images from Figs. 1(f) and 1(g), one can find that after completion of the wetting layer, the Co islands are anchored to the step edge where they nucleate and grow laterally outward from their nucleation sites, expanding in the direction perpendicular to the step edges. Our interpre-

tation is that the islands initially expand on top of flat terraces (on average, terraces are 70 nm wide in the region shown), growing towards the "downhill" direction of the stepped surface and do not expand to cover the adjacent uphill terrace. A few islands are also observed to move slightly away from where they nucleate, again always in the downhill direction.

A similar growth was reported recently for the Cu/Ru(0001) system, where flat-topped islands grow along the downhill direction on stepped surfaces. [26] We find that the growth of Co/Ru(0001) is very similar to the case of Cu/Ru(0001) described in Ref. 26. One difference between the two systems is that our Co islands quickly form after the single wetting layer is completed, while for Cu an additional ML grows and then dewets during the subsequent island formation. Like the Cu islands described in Ref. 26, Co islands are known to have a flat top with the surface oriented in the [0001] direction.[14] When such flat-topped islands initially expand within the same terrace, a 2D growth mode appears to be adopted since the island height does not change. When the islands cross a step edge, however, the part growing in the lowest terrace will increase its height by one atomic step height compared to the part of the island that is on the adjacent upper terrace. By this process, the average height of the island is increased during growth when the lateral island sizes grow beyond substrate terrace widths, even under conditions where new atomic layer nucleation on their flat tops might not take place.

We now present the growth of Co on partially oxygen-terminated Ru(0001). After our usual cleaning procedure involving numerous cycles of flash heating to ≈1300 K in the presence of oxygen, the crystal is flashed one more time without oxygen in the temperature range of ≈1300–1500 K. With the relatively low temperature of the final flash, the remaining oxygen is not completely desorbed. The amount retained depends on the final flashing temperature. Low-energy electron diffraction and scanning tunneling microscopy reveal that the Ru–O forms a 2×2 reconstruction pattern (not shown), indicating the surface is chemisorbed oxygen. We distinguish the observed phase from the physisorbed O–Ru(0001)-2×2 as the physisorbed phase is very mobile even at room temperature and no rhombus shape pattern is found.[17] Figure 3(a) presents a PEEM image of a partially oxygen-terminated substrate with a final flashing around 1400 K. A 10 μm scale, rhombus-shaped pattern is observed. The contrast comes from the workfunction difference between Ru and Ru–O.[18] The brighter background is pure Ru and the geometric patterns are formed by the Ru–O. The formation mechanism is unclear; nevertheless, we can use the patterning as a substrate to study the influence of oxygen on the growth of Co islands on Ru(0001). Figure 3(b) presents the PEEM image for ≈8 MLE of Co grown at ≈800 K. A Co elemental map was obtained by taking an image at the Co $2p-3d$ resonance (778.1 eV) and subtracting a below-resonance background image. In this image, the Co island contrast is enhanced and appears in white. In the pure Ru area, the Co islands form as discussed above. Surprisingly, no Co islands appear in the Ru–O region. The image suggests that Co either has a very low sticking coefficient on the Ru–O region or that the Co grows layer by layer

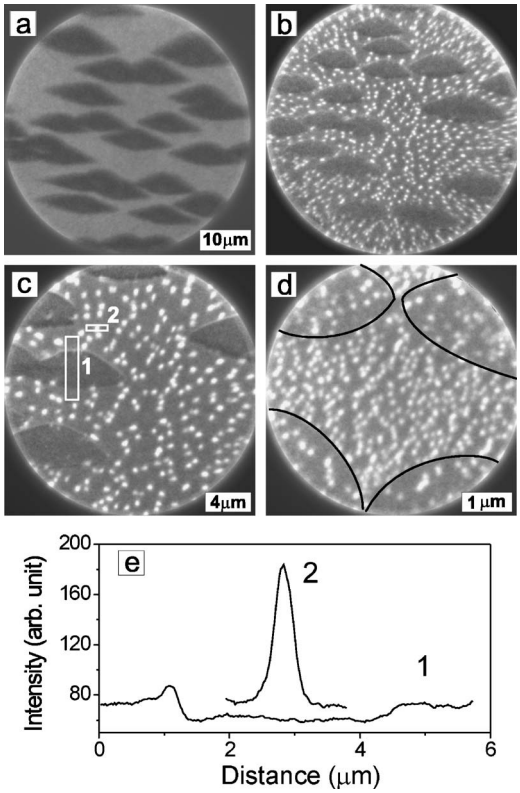

FIG. 3. Typical PEEM image of partially oxidized Ru(0001). The dark rhombus-shaped patterns are Ru oxide and the white region is clean Ru(0001), (b) Co elemental map of ≈8-MLE-Co on partially oxidized Ru(0001), at a deposition temperature of 800 K, (c) a magnified view of image (b), (d) ≈10-MLE Co deposited at 730 K, where the boundaries are marked between the pure Ru and Ru–O areas, (e) line profiles of the Co elemental signal shown in (c), where 1 is across a rhombus, and 2 is across a Co island.

on the Ru–O region at this temperature. This can be distinguished by careful comparison of the contrast of the Co element-specific map. Recalling that Co first forms a 1-ML-wetting layer on the Ru substrate, we can compare the contrast between the Ru–O region and the 1-ML-Co covered region. We find that the Ru–O region is slightly darker than the 1-ML-Co wetting layer that covers the pure Ru region, which indicates that there is almost no Co in the Ru–O region. This can be seen more clearly in the line profiles in Fig. 3(e) across the individual regions marked on Fig. 3(c). We can see that the Co $2p-3d$ resonance intensity on the Ru–O region is lower than the one with 1-ML-Co on Ru. Thus, we conclude that the thickness of the Co on the Ru–O region is much less than 1 ML.

The selective adsorption of the Co nanoislands is possibly related to the large difference in sticking coefficient between Co–RuO and Co–Ru or the difference in binding energy between two interfaces and the high mobility of Co adatoms at the given temperature. If the system is governed by the difference in binding energy and the kinetics of the Co adatoms, one would expect to find Co accumulation near the boundary between these two areas. In our measurement, no such phenomenon is observed, suggesting that the differences in binding energies and the kinetics are not the dominant mecha-

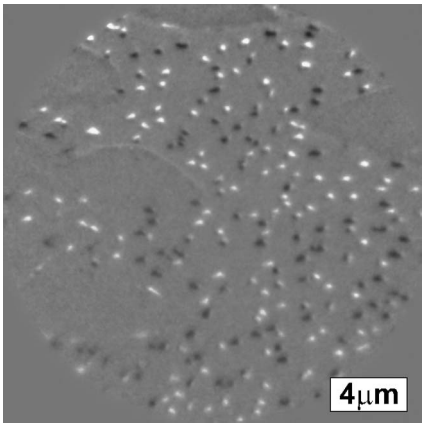

FIG. 4. Magnetic circular dichroism image simultaneously obtained with Fig. 3(c).

nism. For transition metals on most clean oxides, the initial sticking coefficients are close to unity at room temperature (similar to metal-on-metal surfaces) and decrease with increasing temperature.[27] The temperature dependence of the initial sticking coefficient is typically different for transition metals on oxides than on pure metals. On oxides, it usually decreases faster. Therefore, within a certain temperature range, the sticking coefficients can be almost zero on oxide surfaces while their values on metal surfaces are still high, as is observed for Ag on Ru and RuO surfaces.[28] To see if Co behaves similarly, we deposited Co at a slightly lower temperature where it can have a nonzero sticking coefficient on the Ru–O area. Figure 3(d) presents the elemental map of ≈10-MLE-Co deposited at ≈730 K. The lines are inserted to mark the boundaries between the Ru and Ru–O areas (obtained from the below-resonance image where the boundary contrast is less disturbed by the Co contrast). In comparison with Fig. 3(c), smaller and denser islands are found on the pure Ru area, due to the lower growth temperature. In the area of the Ru-O, islands with similar sizes also form but with much less density than occurs on the pure Ru region. The fact that islands with similar size but different density are found in the Ru and Ru–O areas provides evidence for different temperature dependent sticking coefficients of the Co to the Ru and Ru–O surfaces. This explains how the Co islands form selectively on the partially oxidized Ru surface at ≈800 K. The selectivity suggests that the oxygen-patterned substrate can serve as a mask for the selected deposition of metallic islands.

Figure 4 presents the magnetic image of the same area as in Fig. 3(c). The image was obtained using magnetic circular dichroism as a difference of two on-resonance images taken with left- and right-circularly polarized x-rays. Most of the individual islands are imaged in a uniform shade of gray, suggesting that they are in a single domain magnetic state. The various shades of gray indicate that the islands are magnetized in the sample plane as only two shades of contrast could exhibit in the case that the islands are magnetized perpendicular to the surface. This is in agreement with our previous magneto-optical Kerr effect and magnetic force microscopy measurements.[29,30] The different shade of gray of each island also suggests that the magnetization of the ensemble of islands is randomly distributed. When separation between the islands is small, the islands could couple to each other through magneto static interactions.[30] In the extreme case, when two islands are merged together, two domain structure with opposite magnetization can also be found.[31] No magnetic contrast is found in the 1-ML-Co wetting layer covering the pure Ru region which is probably related to the fact that its Curie temperature is below room temperature. With this, we also suppose there is no significant magnetic communication through the wetting layer. We did not observe any magnetic contrast in the Ru–O region either. This also provides additional evidence that there is no Co in the Ru–O region in Fig. 3(c), since an 8-ML continuous film of Co would have to be magnetic at room temperature.

IV. CONCLUSIONS

In summary, in combination with both low energy electron microscopy and photoemission electron microscopy, we investigated Co growth in the temperature range of 700–850 K on a pure and partially oxidized Ru(0001) substrate. On the pure Ru substrate, we find that Co first forms a 1-ML wetting layer followed by an abrupt nucleation of islands. A 10-μm scale, Ru–O rhombus-shaped pattern is formed when the substrate is prepared to retain some residual oxygen. Co forms islands with different densities in the Ru and Ru-O regions at ≈730 K, while at ≈800 K , Co islands only form on the pure Ru region. We attribute this selectivity to the existence of different temperature dependences of the sticking coefficients for the two surfaces.

ACKNOWLEDGMENTS

This work was supported by the US DOE BES-Materials Sciences under Contract No. W-31-109-ENG-38 at ANL and No. DE-AC03-76SF00098 at LBNL. S.D.B. and H.F.D. acknowledge support from the ANL-University of Chicago Consortium for Nanoscience Research (CNR).

*Electronic address: hfding@gmail.com

[1] G. M. Whitesides and B. Grzybowski, Science **295**, 2418 (2002).
[2] P. Politi, G. Grenet, A. Marty, A. Ponchet, and J. Villain, Phys. Rep. **324**, 271 (2000).
[3] H. J. Elmers, J. Hauschild, H. Höche, U. Gradmann, H. Bethge, D. Heuer, and U. Köhler, Phys. Rev. Lett. **73**, 898 (1994).
[4] F. J. Himpsel, T. Jung, and J. E. Ortega, Surf. Rev. Lett. **4**, 371 (1997).
[5] J. Shen, R. Skomski, M. Klaua, H. Jenniches, S. S. Manoharan, and J. Kirschner, Phys. Rev. B **56**, 2340 (1997).
[6] D. Li, B. R. Cuenya, J. Pearson, S. D. Bader, and W. Keune, Phys. Rev. B **64**, 144410 (2001).

[7] P. Gambardella, A. Dallmeyer, K. Maiti, M. C. Malagoli, W. Eberhardt, K. Kern, and C. Carbone, Nature (London) **416**, 301 (2002).
[8] H. Brune, M. Giovannini, K. Bromann, and K. Kern, Nature (London) **394**, 451 (1998).
[9] E. D. Tober, R. C. F. Farrow, R. F. Marks, G. Witte, K. Kalki, and D. D. Chambliss, Phys. Rev. Lett. **81**, 1897 (1998).
[10] D. Li, V. Diercks, J. Pearson, J. S. Jiang, and S. D. Bader, J. Appl. Phys. **85**, 5285 (1999).
[11] K. Meinel, H. Wolter, C. Ammer, and H. Neddermeyer, Surf. Sci. **402**, 299 (1998).
[12] V. Repain, G. Baudot, H. Ellmer, and S. Rousset, Mater. Sci. Eng., B **96**, 178 (2002).
[13] H. Ellmer, V. Repain, M. Sotto, and S. Rousset, Surf. Sci. **511**, 183 (2002).
[14] C. Yu, D. Li, J. Pearson, and S. D. Bader, Appl. Phys. Lett. **78**, 1228 (2001).
[15] H. Over, Y. D. Kim, A. P. Seitsonen, S. Wendt, E. Lundgren, M. Schmid, P. Varga, A. Morgante, and G. Ertl, Science **287**, 1474 (2000).
[16] H. Over and A. P. Seitsonen, Science **297**, 2003 (2002).
[17] A. K. Schmid, R. Q. Hwang, and N. C. Bartelt, Phys. Rev. Lett. **80**, 2153 (1998).
[18] A. Böttcher, B. Krenzer, H. Conrad, and H. Niehus, Surf. Sci. **466**, L811 (2000).
[19] A. Böttcher, U. Starke, H. Conrad, R. Blume, H. Niehus, L. Gregoratti, B. Kaulich, A. Barinov, and M. Kiskinova, J. Chem. Phys. **117**, 8104 (2002).
[20] M. Todorova, W. X. Li, M. V. Ganduglia-Pirovano, C. Stampfl, K. Reuter, and M. Scheffler, Phys. Rev. Lett. **89**, 096103 (2002).
[21] E. Bauer, Surf. Rev. Lett. **5**, 1275 (1998).
[22] M. S. Altman, W. F. Chung, and C. H. Liu, Surf. Rev. Lett. **5**, 1129 (1998).
[23] J. Stöhr, H. A. Padmore, S. Anders, T. Stammler, and M. R. Scheinfein, Surf. Rev. Lett. **5**, 1297 (1998).
[24] H. Hopster and H. P. Oepen, *Magnetic Microscopy of Nanostructures* (Springer-Verlag, New York, 2004), pp. 1–28.
[25] L. Vitos, A. V. Ruban, H. L. Skriver, and K. Kollár, Surf. Sci. **411**, 186 (1998).
[26] W. L. Ling, T. Giessel, K. Thürmer, R. Q. Hwang, N. C. Bartelt, and K. F. McCarty, Surf. Sci. **570**, L297 (2004).
[27] C. T. Campbell, Surf. Sci. Rep. **27**, 1 (1997).
[28] D. G. V. Campen and J. Hrbek, J. Phys. Chem. **99**, 16389 (1995).
[29] C. Yu, D. Li, J. Pearson, and S. D. Bader, Appl. Phys. Lett. **79**, 3848 (2001).
[30] C. Yu, J. Pearson, and D. Li, J. Appl. Phys. **91**, 6955 (2002).
[31] H. F. Ding, A. K. Schmid, D. Li, K. Y. Guslienko, and S. D. Bader, Phys. Rev. Lett. **94**, 157202 (2005).